ARTICLE

EZH2 regulates a SETDB1/ΔNp63α axis via RUNX3 to drive a cancer stem cell phenotype in squamous cell carcinoma

Seamus Balinth[1,2], Matthew L. Fisher[1], Yon Hwangbo[1], Caizhi Wu[1], Carlos Ballon[1], Xueqin Sun[1] and Alea A. Mills[1]✉

Enhancer of zeste homolog 2 (EZH2) and SET domain bifurcated 1 (SETDB1, also known as ESET) are oncogenic methyltransferases implicated in a number of human cancers. These enzymes typically function as epigenetic repressors of target genes by methylating histone H3 K27 and H3-K9 residues, respectively. Here, we show that EZH2 and SETDB1 are essential to proliferation in 3 SCC cell lines, HSC-5, FaDu, and Cal33. Additionally, we find both of these proteins highly expressed in an aggressive stem-like SCC sub-population. Depletion of either EZH2 or SETDB1 disrupts these stem-like cells and their associated phenotypes of spheroid formation, invasion, and tumor growth. We show that SETDB1 regulates this SCC stem cell phenotype through cooperation with ΔNp63α, an oncogenic isoform of the p53-related transcription factor p63. Furthermore, EZH2 is upstream of both SETDB1 and ΔNp63α, activating these targets via repression of the tumor suppressor RUNX3. We show that targeting this pathway with inhibitors of EZH2 results in activation of RUNX3 and repression of both SETDB1 and ΔNp63α, antagonizing the SCC cancer stem cell phenotype. This work highlights a novel pathway that drives an aggressive cancer stem cell phenotype and demonstrates a means of pharmacological intervention.

Oncogene (2022) 41:4130–4144; https://doi.org/10.1038/s41388-022-02417-4

INTRODUCTION

Squamous cell carcinomas (SCCs) are prominent cancers emanating from the epithelia of various organs including the skin, lungs, esophagus, cervix, urinary tract, and mucous membranes of the head and neck [1]. Human papilloma virus, Epstein-Barr virus, UV radiation, tobacco use, alcohol consumption, and acid reflux disease are environmental contributors to these malignancies [2–7]. In addition to chemotherapy and radiotherapy [8, 9], targeted therapies have been used to varying success in SCC patients, with drugs such as cetuximab, afatinib, erlotinib, pembrolizumab, and nivolumab targeting processes critical to cancer progression such as EGFR signaling and immune evasion via lymphocyte PD-1 engagement [10, 11]. These targeted approaches have improved patient outcome, giving credence to the notion that targeting specific SCC oncogenes is a viable approach for improving upon existing patient regimens. Despite these advances in targeted therapy, survival rates remain poor; therefore, there is a dire need for more effective therapeutic options for SCC patients. Emerging evidence implicates cancer stem cells (CSCs) as promoters of advanced SCC through enhancing tumor growth, invasion, and drug resistance [12, 13]. Thus, targeted therapies against oncogenes vital to CSC maintenance hold high therapeutic promise for preferentially eradicating the sub-population of tumor cells essential to SCC.

In recent work, we show we can enrich for stem-like cancer cells by growth in non-attached conditions as spheroids [14]. Furthermore, we define the p63 isoform ΔNp63α as a key mediator of the aggressive CSC phenotype in SCC. p63 is a p53-related transcription factor that regulates key cellular functions including proliferation, apoptosis, and differentiation in numerous tissues. Its expression is critical in development, as seen in mouse models with defects in limb growth and epidermal structures. Importantly, p63 is required for the development of stratified epithelia and the maintenance of epithelial stem cells [15, 16]. *p63* mutations are responsible for seven human developmental disease syndromes in which patients have defects in ectodermal lineages such as the skin, tongue and palate [17]. The diversity of these roles is largely accounted for by the expression of different p63 isoforms [18]. Transcription from different *p63* promoters yield N-terminally truncated forms of the protein (ΔNp63) or proteins containing an N-terminal 'p53-like' transactivation domain (TAp63) [19]. These distinct isoform classes can also be alternatively spliced, such that both the ΔN- and the TA-p63 classes may generate three different major isoforms (alpha, beta, or gamma) that differ based on their C-termini. Our prior work indicates that ΔNp63α drives the stem-like population of SCC cells [14].

Previous work connects chromatin remodeling proteins to ΔNp63 regulation [14, 18], implicating this class of proteins as a viable target for therapeutic intervention. Here, we investigate the role of the histone methyltransferases EZH2 and SETDB1 as regulators of ΔNp63α and the aggressive CSC phenotype.

SETDB1 functions as an epigenetic repressor of target genes via tri-methylation of histone H3K9 [20]. SETDB1 is associated with numerous cancers, and increases in SETDB1 expression correlates with cancer progression and metastasis [21]. In the context of breast cancer, SETDB1 directly binds ΔNp63α and promotes oncogenesis [22].

[1]Cold Spring Harbor Laboratory, Cold Spring Harbor, NY, USA. [2]Molecular and Cellular Biology Program, Stony Brook University, Stony Brook, NY, USA. ✉email: mills@cshl.edu

Received: 29 January 2022 Revised: 6 July 2022 Accepted: 8 July 2022
Published online: 21 July 2022

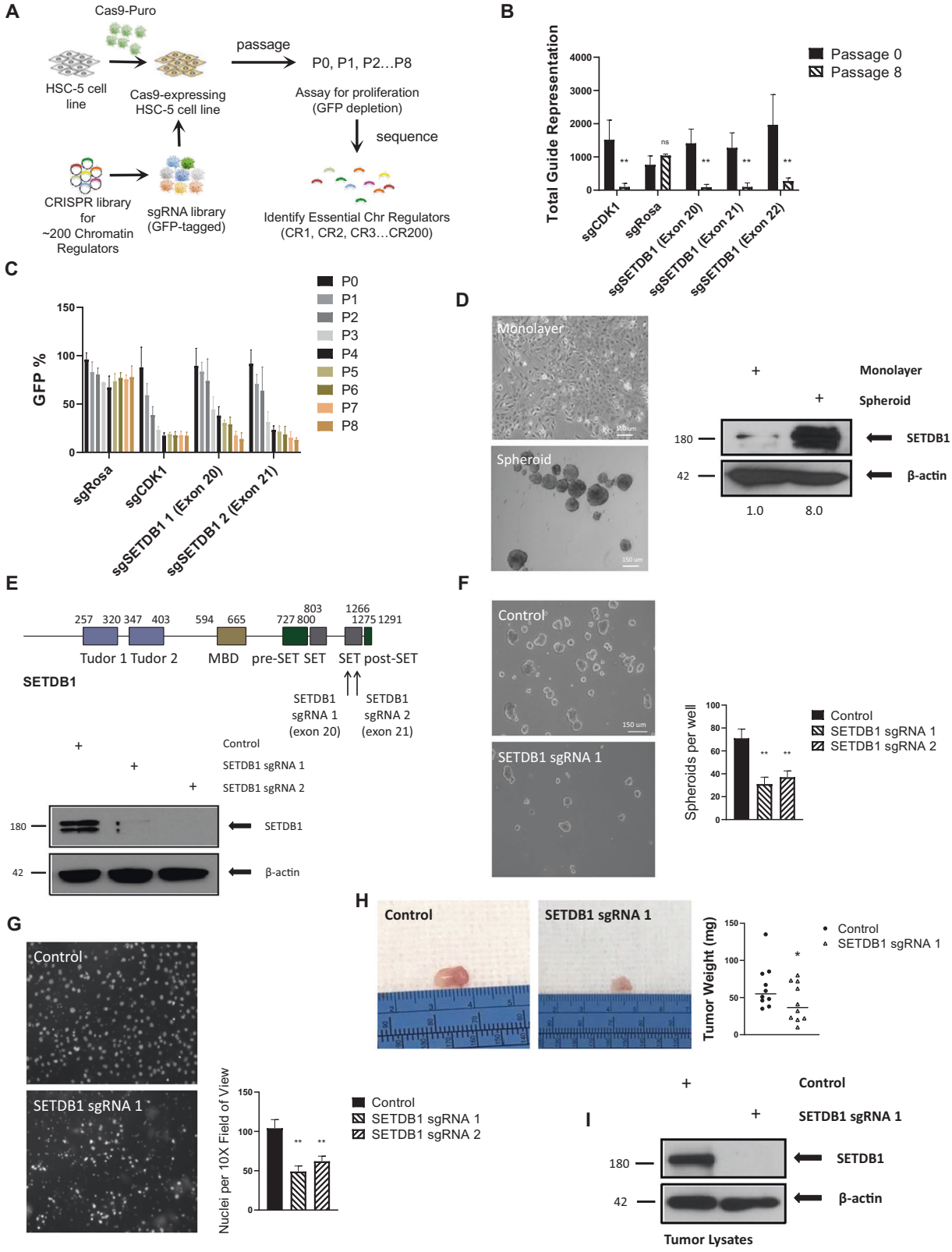

EZH2 is a histone H3K27 methyltransferase that functions as the catalytic component of polycomb repressive complex 2 (PRC2) that epigenetically silences target genes [23]. EZH2 has been studied as a driver of an abundance of cancers [24, 25], and specifically of SCCs via pSTAT3 regulation [26] which we have also connected directly to ΔNp63α [14]. The emergence of EZH2 inhibitors [27] promises to capitalize on this key enzyme as a viable target for treating SCC.

This work builds on our previous efforts to understand p63 as a regulator of SCC by delineating an interaction with SETDB1 that is

Fig. 1 SETDB1 regulates a cancer stem cell phenotype in SCC. A, **B** Domain-focused CRISPR library screening revealed SETDB1 to be required for proliferation of HSC-5 cells when grown as a monolayer. **C** Guide RNAs targeting exons 20 and 21 of *SETDB1* were cloned into a GFP expression vector, and GFP depletion was tracked over 8 passages in monolayer culture. **D** HSC-5 cells were grown in non-attachment (spheroid) conditions for 10 days (left), and protein lysates were collected to perform western blotting for SETDB1, which was then quantified (right). **E** Two guide RNAs were used to target SETDB1 (top) and induce CRISPR-mediated depletion in HSC-5 cells, which was confirmed by western blotting (bottom). **F** Control and SETDB1-depleted cells were then grown in spheroid conditions for 10 days. Total spheres were counted at day 10. **G** Control and SETDB1-depleted cells were also plated for transwell cell invasion assays. The basement membrane of transwell inserts were fixed, DAPI stained and imaged after 24 h of invasion. **H** Control and SETDB1-depleted HSC-5 cells were also injected subcutaneously into the the rear flanks of nude mice at concentrations of 2.5×10^5 cells per injection. Tumors were collected and weighed once diameters eclipsed 8 mm by caliper measurement. **I** Protein lysates were then collected and western blotting was used to confirm SETDB1 depletion. Student's *t* tests were used to measure statistical significance (ns not significant, **p* value < 0.10, ***p* value < 0.05). The average of three biological experiments is plotted for each experiment, except for the CRISPR screen which was run in duplicate. Each biological replicate was run in triplicate.

highly relevant to a stem-like SCC phenotype, and also by investigating EZH2 as an upstream regulator of ΔNp63α/SETDB1 signaling. We discover the transcription factor RUNX3 as an intermediate component of the pathway that is repressed by EZH2. RUNX3 is a tumor suppressor implicated in apoptosis and inhibition of proliferation and invasion in several cancers [28, 29]. Here we show that RUNX3 is repressed by EZH2's methyltransferase function in SCC, and when activated, RUNX3 significantly compromises ΔNp63α and SETDB1 expression, thereby impairing the cancer stem-like SCC sub-population.

RESULTS

SETDB1 is required for SCC cell survival and maintenance of stem-like cancer cells

We previously connected chromatin remodeling proteins to SCC progression and maintenance of stem-like cancer cells [14, 30]. Here, we implemented a CRISPR screen in SCC cells with short guide RNAs (sgRNAs) targeting exons that encode the functional domains of nearly 200 chromatin regulating proteins [31]. Cas9 was stably expressed in HSC-5 cells using a lentiviral transduction. The sgRNA library was then introduced to the cell population, and the cells were passaged 8 times, with genomic DNA being collected for sequencing at passage 0 and passage 8 (Fig. 1A).

From the screening library of pooled sgRNAs, *SETDB1* was targeted by 9 guides RNAs to exons 20, 21, and 22, which all encode the catalytic SET domain. We observed significant depletion of the guides from passage 0 to passage 8, similar to what was observed for guides targeting the positive control, CDK1 (Fig. 1B). To confirm that *SETDB1* was essential for the proliferation of HSC-5 cells, we cloned individual sgRNAs specific to exons 20 and 21 of *SETDB1* into GFP expression vectors and monitored GFP depletion for 8 passages, spanning 30 days; these sgRNAs were significantly depleted from the cell population at the final passage, whereas GFP expression for the negative control (targeting Rosa26 locus) remained stable throughout the assay (Fig. 1C). We validated this depletion profile in Cal33 and FaDu SCC cell lines as well (Supplementary Fig. 1A). Thus, SETDB1 has an important role in cell proliferation for SCC cells grown in 2-dimensions (monolayer). Given the link between chromatin remodelers and cancer stemness, we investigated the role of SETDB1 on the SCC CSC phenotype by enriching for stem-like cells through non-attachment (spheroid) growth [14]. Following the spheroid growth of HSC-5 cells, a significant enrichment of SETDB1 protein was observed (Fig. 1D). SETDB1 protein was also seen to increase in expression in FaDu and Cal33 cells following spheroid growth, although no increase was observed at the mRNA level for any cell line (Supplementary Fig. 1B, C). CRISPR-Cas9 was then used to generate SETDB1-depleted cells, prior to spheroid growth assays (Fig. 1E). We observed a significant reduction in spheroid formation upon SETDB1 loss following 10 days of non-attachment growth (Fig. 1F). We also investigated the role of SETDB1 in cell invasion and tumor growth, properties correlating with the SCC CSC phenotype [14]. SETDB1 depletion caused a significant decrease in invasion through Matrigel (Fig. 1G). SETDB1-depleted Cal33 and FaDu cell lines were also established (Supplementary Fig. 1D), and plated for spheroid formation and invasion assays. SETDB1 loss resulted in significant decreases in spheroid formation and invasion (Supplementary Fig. 1E, F). Lastly, we established tumor xenograft mouse models by subcutaneous injection of SETDB1-depleted HSC-5 cells which resulted in reduced tumor size compared to controls (Fig. 1H). Western blotting was used to confirm the loss of SETDB1 in the extracted tumors (Fig. 1I). Thus, the SETDB1 methyltransferase is essential to CSC-associated phenotypes of SCC.

ΔNp63α is a critical mediator of SETDB1 function in stem-like SCC cells

Considering the necessity of SETDB1 in promoting a CSC phenotype (see Fig. 1E–H), and its connection to ΔNp63α [22], an oncogenic isoform of p63 that is highly expressed in SCC [32], we sought to identify the extent to which ΔNp63α is required for SETDB1-influenced SCC biology. We performed western blotting for p63 in SETDB1-depleted HSC-5 cells. ΔNp63α expression decreased significantly following SETDB1 loss (Fig. 2A), which we confirmed in FaDu and Cal33 cells (Supplementary Fig. 1B). By assessing *ΔNp63* mRNA expression via RT-qPCR following SETDB1 depletion, we found a greater than twofold reduction in *ΔNp63* mRNA abundance (Fig. 2B). Thus, SETDB1 is required in HSC-5 cells to maintain ΔNp63α expression at the protein and mRNA levels. To determine whether SETDB1 affects the aggressive CSC-associated phenotype in a ΔNp63α-dependent manner, we transduced SETDB1-depleted HSC-5 cells with a ΔNp63α expression vector to rescue endogenous p63 loss (Fig. 2C). ΔNp63α expression rescued the ability of SETDB1 depletion to compromise both spheroid formation and invasion (Fig. 2D, E). Furthermore, our co-immunoprecipitation experiments indicated that ΔNp63α and SETDB1 directly interact (Fig. 2F). These findings indicate that ΔNp63α is essential for SETDB1-mediated cancer stem cell phenotypes in SCC.

ΔNp63α regulates SETDB1 expression

Having established the strong influence of SETDB1 on ΔNp63α expression and maintenance of CSC phenotypes, we assessed the possibility of feedback from ΔNp63α to SETDB1 by depleting ΔNp63α and monitoring changes in SETDB1 expression. Indeed, CRISPR-mediated depletion of ΔNp63α reduced SETDB1 protein (Fig. 3A). Thus, ΔNp63α and SETDB1 acted to promote expression of each other. However, RT-qPCR analysis of *SETDB1* following ΔNp63α depletion did not significantly alter *SETDB1* mRNA levels, indicating that ΔNp63α affected SETDB1 expression at the protein level (Fig. 3B). This finding was bolstered by p63 ChIP-seq in HSC-5 cells, where p63 peaks were found at specific regions, such as upstream of the ΔNp63 promoter, consistent with previous findings [33–37]. We did not observe p63 binding at the *SETDB1* gene (Supplementary Fig. 2A).

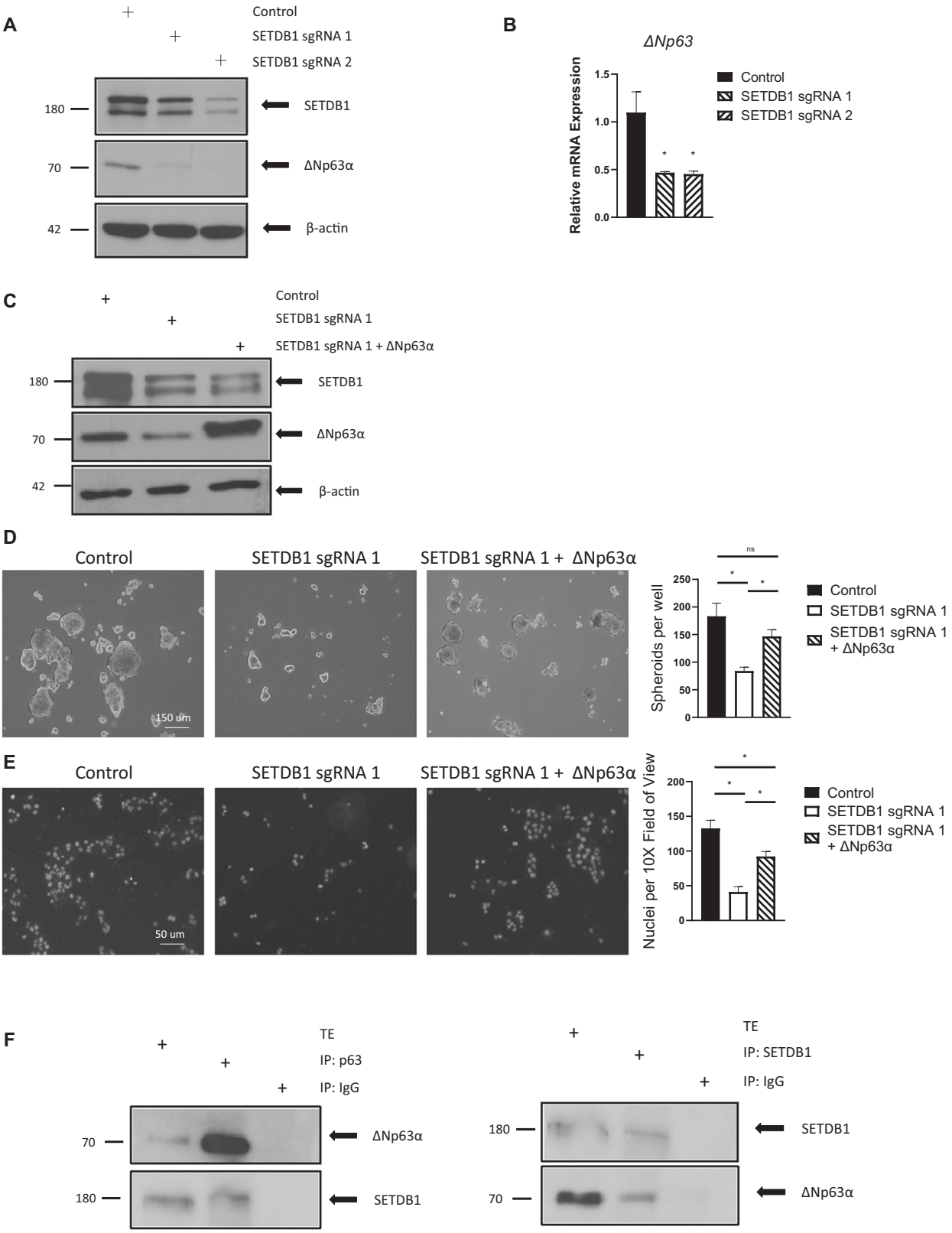

Fig. 2 SETDB1 regulates an SCC CSC phenotype via ΔNp63α. A Two SETDB1 guide RNAs were used to deplete SETDB1 in Cas9-expressing HSC-5 cells. Western blotting was then used to detect ΔNp63α expression in SETDB1-depleted cell lines. **B** ΔNp63 mRNA expression was assessed in SETDB1-depleted cells using RT-qPCR. **C** A ΔNp63α expression vector was introduced in SETDB1-depleted cell lines, and rescue of ΔNp63α protein expression was confirmed by western blot. Rescued cell lines were compared to control cells and SETDB1-depleted cells in (**D**) spheroid formation and (**E**) cell invasion assays. **F** Day 10 spheroid lysates were collected and co-immunoprecipitation was performed for SETDB1 and p63. Student's *t* tests were used to measure statistical significance (ns not significant, **p* value < 0.05). The average of three biological experiments is plotted for each experiment. Each biological replicate was run in triplicate.

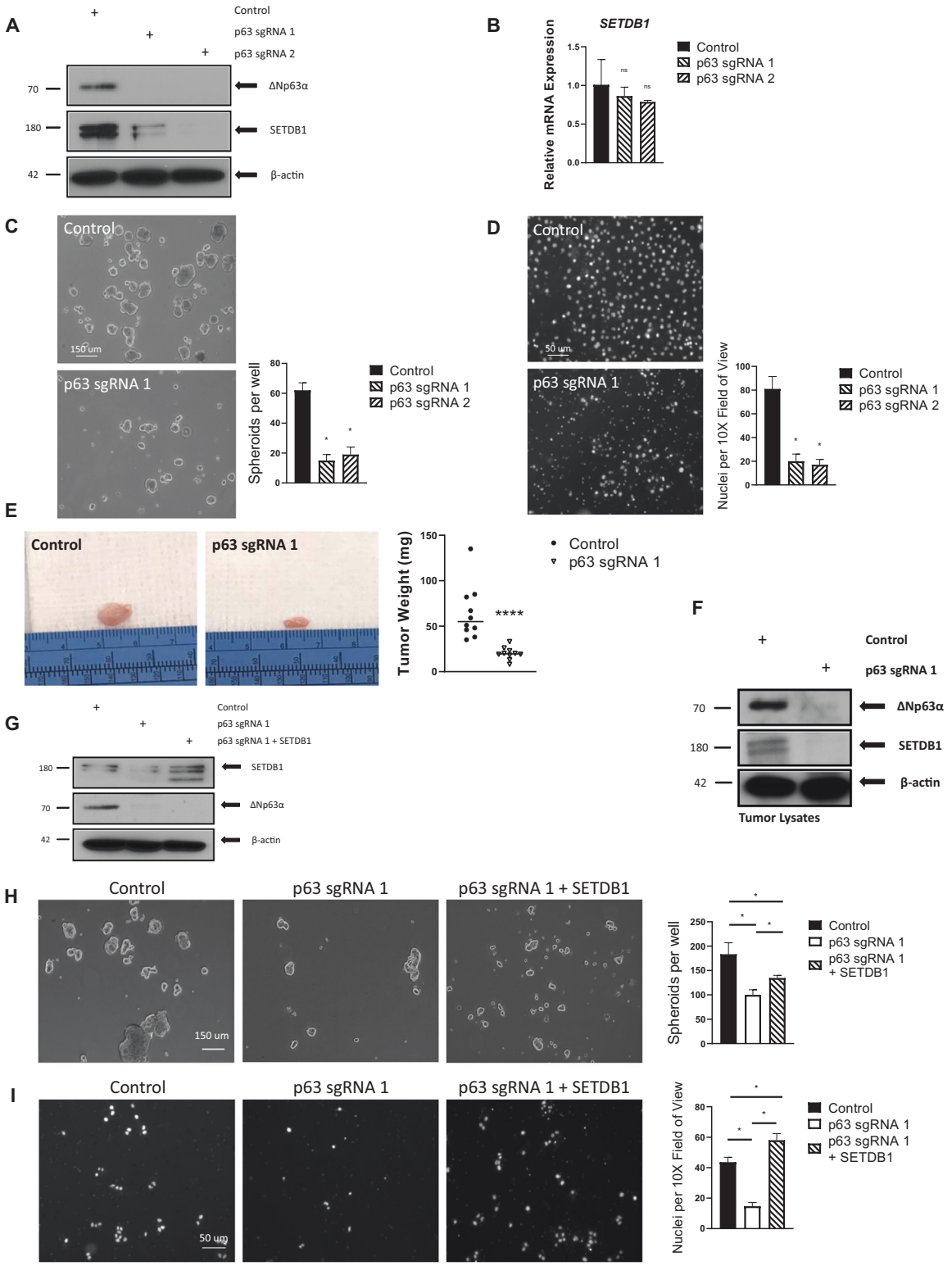

Fig. 3 ΔNp63α regulates SETDB1 to influence the SCC CSC phenotype. A Two guide RNAs were used to deplete p63 in Cas9-expressing HSC-5 cells. ΔNp63α and SETDB1 expression were examined by western blotting. **B** RT-qPCR analysis of *SETDB1* was carried out in ΔNp63α-depleted and control cells. **C** Control and ΔNp63α-depleted HSC-5 cells were then plated for spheroid formation and (**D**) invasion assays. **E** Control and ΔNp63α-depleted cells were also injected subcutaneously into the the rear flanks of nude mice at concentrations of 2.5×10^5 cells per injection. Tumors were collected and weighed once diameters eclipsed 8 mm by caliper measurement. **F** Protein lysates were then collected and western blotting was used to confirm ΔNp63α and SETDB1 depletion. **G** SETDB1 was reintroduced into ΔNp63α-depleted HSC-5 cells via a SETDB1 expression vector. Rescue of SETDB1 expression was confirmed by western blot, and the effect of the rescue was measured on (**H**) spheroid formation and (**I**) invasion compared to control and ΔNp63α-depleted cells. Student's *t* tests were used to measure statistical significance (ns not significant, **p* value < 0.05, *****p* value < 0.0001). The average of three biological experiments is plotted for each experiment. Each biological replicate was run in triplicate.

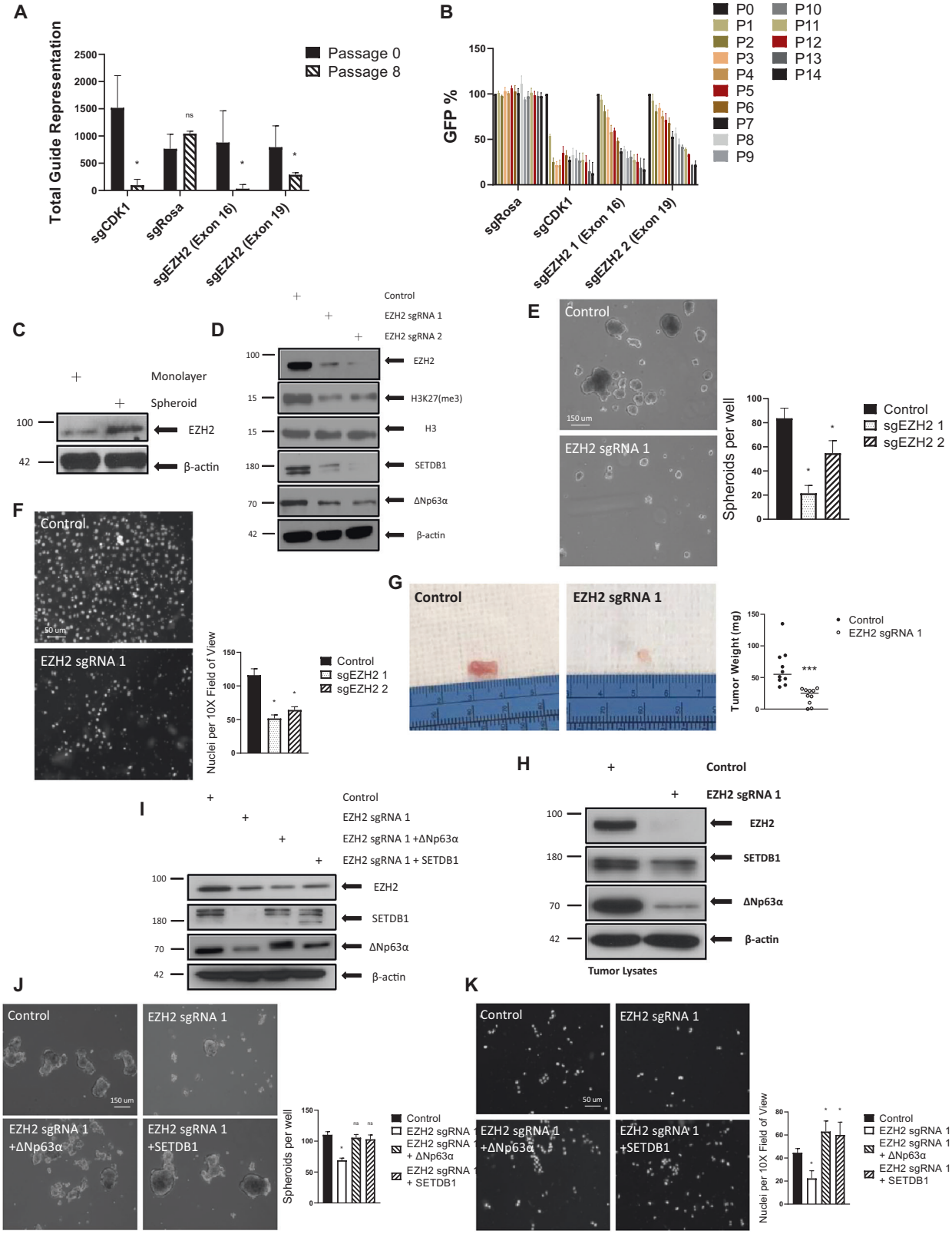

SETDB1 binding partners such as ATF7IP play a role in shielding SETDB1 from degradation at the proteasome [38]. To determine if ΔNp63α physically stabilizes SETDB1 in a similar manner, we treated ΔNp63α-depleted cells with the proteasome inhibitor MG132, to test whether SETDB1 expression would be restored. MG132 treatment however, did not rescue SETDB1 expression in ΔNp63α-depleted cell lines, indicating that ΔNp63α regulates SETDB1 protein through a mechanism that is independent from preventing proteasomal degradation (Supplementary Fig. 2B).

Fig. 4 EZH2 regulates SETDB1 and ΔNp63α, and their corresponding phenotypes. A Domain-focused CRISPR library screening revealed SETDB1 to be required for proliferation of HSC-5 cells when grown as a monolayer. **B** Guide RNAs targeting exons 16 and 19 of *EZH2* were cloned into a GFP expression vector, and GFP depletion was tracked over 14 passages in monolayer culture. **C** Protein lysates were collected from monolayer and spheroid derived HSC-5 cells after 10 days of growth, and blotted for EZH2. **D** Two guide RNAs were used to deplete EZH2 in Cas9-expressing HSC-5 cells. Western blotting was used to examine expression of EZH2, tri-methyl H3K27 (a mark of EZH2 activity), SETDB1, and ΔNp63α. Additionally, control and EZH2-depleted HSC-5 cells were plated for (**E**) spheroid formation and (**F**) invasion assays. **G** Control and EZH2-depleted cells were also injected subcutaneously into the the rear flanks of nude mice at concentrations of 2.5×10^5 cells per injection. Tumors were collected and weighed once diameters eclipsed 8 mm by caliper measurement. **H** Protein lysates were then collected and western blotting was used to confirm EZH2, ΔNp63α, and SETDB1 depletion. **I** EZH2-depleted HSC-5 cells were rescued with either ΔNp63α or SETDB1 expression vectors and examined by western blot. Rescued cell lines were then plated for (**J**) spheroid formation and (**K**) invasion assays alongside control and EZH2-depleted conditions. Student's *t* tests were used to measure statistical significance (ns not significant, **p* value < 0.05, ****p* value = 0.0001). The average of three biological experiments is plotted for each experiment. Each biological replicate was run in triplicate.

Considering ΔNp63α's regulatory role on SETDB1, we asked whether the proteins had an overlapping biological impact on SCC. Using spheroid formation and invasion assays, we found that ΔNp63α-depleted HSC-5 cells performed significantly poorer than control cells (Fig. 3C, D), a finding we confirmed in FaDu and Cal33 cells (Supplementary Fig. 3A–C). Furthermore, we generated tumor xenografts from ΔNp63α-depleted HSC-5 cells and observed significantly smaller tumors than controls, again mirroring the effect seen from SETDB1 depletion (Fig. 3E). Western blotting confirmed loss of ΔNp63α and SETDB1 in these tumors (Fig. 3F).

As shown in Fig. 2C–E, SETDB1 enacts its effect on a SCC CSC phenotype in a ΔNp63α-dependent manner. To test if the inverse was true, we rescued ΔNp63α-depleted HSC-5 cells with a SETDB1 expression vector (Fig. 3G). SETDB1 expression partially rescued the ΔNp63α-depletion phenotype of spheroid formation, and fully rescued the invasion ability of these cells (Fig. 3G, H). These findings indicate that SETDB1 is an important mediator of ΔNp63α's effect on the SCC CSC phenotype.

EZH2 regulates a SCC CSC phenotype through ΔNp63α and SETDB1

ΔNp63α and SETDB1 cooperating to regulate critical phenotypes in SCC is an important concept that required further elucidation. The knowledge that these two essential oncoproteins regulate each other's expression opened the door to other transcription factors or chromatin remodelers that participate in ΔNp63α/SETDB1 function. Due to our previous work connecting the PRC2 component EZH2 to ΔNp63α [14], we investigated a possible role for EZH2 in the regulation of ΔNp63α/SETDB1 signaling.

EZH2 scored as essential in our domain-focused CRISPR screen (Fig. 4A). Validation with individual GFP-tagged sgRNAs confirmed that EZH2 depletion correlated with decreased cell proliferation over the course of 14 passages in monolayer cell culture (Fig. 4B), a finding we confirmed in FaDu and Cal33 cells (Supplementary Fig. 4A). To determine if EZH2 was elevated in spheroids with SETDB1 and ΔNp63α, we used western blotting and found EZH2 was elevated in spheroid culture (Fig. 4C). This increase was also observed in FaDu and Cal33 cells, and confirmed at the mRNA level in all three cell lines (Supplementary Fig. 4B, C). Depletion of EZH2 expression with two different sgRNAs and western blotting for EZH2, H3K27me3, ΔNp63α and SETDB1 in EZH2-depleted HSC-5 cells indicated that both EZH2 and its catalytic mark, H3K27me3 were reduced. Furthermore, we observed significant decreases in both ΔNp63α and SETDB1 expression (Fig. 4D).

Considering EZH2 regulates ΔNp63α and SETDB1, we expected that EZH2-depleted cells would be similarly compromised in spheroid formation and invasion to those with the loss of ΔNp63α or SETDB1. Indeed, spheroid and invasion assays indicated that EZH2 loss significantly impaired cell performance relative to controls (Fig. 4E, F). CRISPR-mediated depletion of EZH2 in FaDu and Cal33 cell lines caused similar decreases in both ΔNp63α and SETDB1 (Supplementary Fig. 4D). These cells also displayed a decreased ability to form spheroids and to invade (Supplementary Fig. 4E, F). Additionally, EZH2-depleted HSC-5 cells generated significantly smaller tumors (Fig. 4G). Western blotting of tumor lysates showed a loss ΔNp63α and SETDB1 expression in EZH2-deficient tumors (Fig. 4H).

To explore whether EZH2's regulation of ΔNp63α and SETDB1 was responsible for its effect on the aggressive SCC CSC phenotype, we created rescue HSC-5 cell lines by expressing SETDB1 or ΔNp63α cDNAs in EZH2-depleted cells (Fig. 4I). Indeed, reintroduction of either target efficiently rescued spheroid formation and invasion resulting from EZH2 loss (Fig. 4J, K). These findings demonstrate a mechanism whereby EZH2 regulates a CSC phenotype in SCC via regulation of ΔNp63α and SETDB1.

EZH2 regulates ΔNp63α and SETDB1 via its methyltransferase activity

To assess the potential of the EZH2/ΔNp63α/SETDB1 axis as a therapeutic target, we utilized GSK126 and EPZ-6438 which act as SAM-competitive inhibitors of EZH2 methyltransferase activity [27]. HSC-5 cells were treated with either GSK126 or EPZ-6438 and western blotting for ΔNp63α, SETDB1, EZH2, and EZH2's catalytic mark (H3K27me3) was performed. Both inhibitors effectively inhibited EZH2's activity, as shown by the loss of H3K27me3, while not impacting EZH2 levels (Fig. 5A, B). Both EZH2 inhibitors depleted ΔNp63α and SETDB1, indicating that EZH2 regulates these targets via its methyltransferase function. Moreover, GSK126 treatment inhibited spheroid formation and invasion in HSC-5 cells (Fig. 5C, D), phenotypes that were also disrupted by EPZ-6438 treatment (Fig. 5E, F). These findings were confirmed in FaDu and Cal33 cells by blotting for ΔNp63α, SETDB1, EZH2, and H3K27me3 following GSK126 or EPZ-6438 treatment (Supplementary Fig. 5A, B). Concomitantly, spheroid formation and invasion were significantly compromised following GSK126 treatment (Supplementary Fig. 5C, D), and also following EPZ-6438 treatment (Supplementary Fig. 5E, F).

Considering pharmacological inhibition of EZH2 decreased ΔNp63α and SETDB1, we attempted to rescue the effect of GSK126 treatment on the SCC CSC phenotype. HSC-5 cells were transduced with SETDB1 or ΔNp63α cDNAs to force expression, and then treated with either DMSO or GSK126. Rescues of protein expression (Fig. 5G) spheroid formation (Fig. 5H) and invasion (Fig. 5I) were evident. GSK126 treatment did not significantly impact spheroid formation or invasion following forced expression of either ΔNp63α or SETDB1, indicating that stabilization of either target alone following inhibition of EZH2's catalytic activity was sufficient to restore the SCC CSC phenotype. Thus, EZH2 regulates expression of ΔNp63α and SETDB1 through its methyltransferase function, and the activation of at least one of these targets is critical to EZH2 exerting an effect on spheroid formation and invasion in SCC.

EZH2-mediated repression of RUNX3 indirectly activates ΔNp63α, SETDB1, and promotes a SCC CSC phenotype

As the catalytic component of PRC2, EZH2 is canonically responsible for suppressing target genes [23]. To identify a

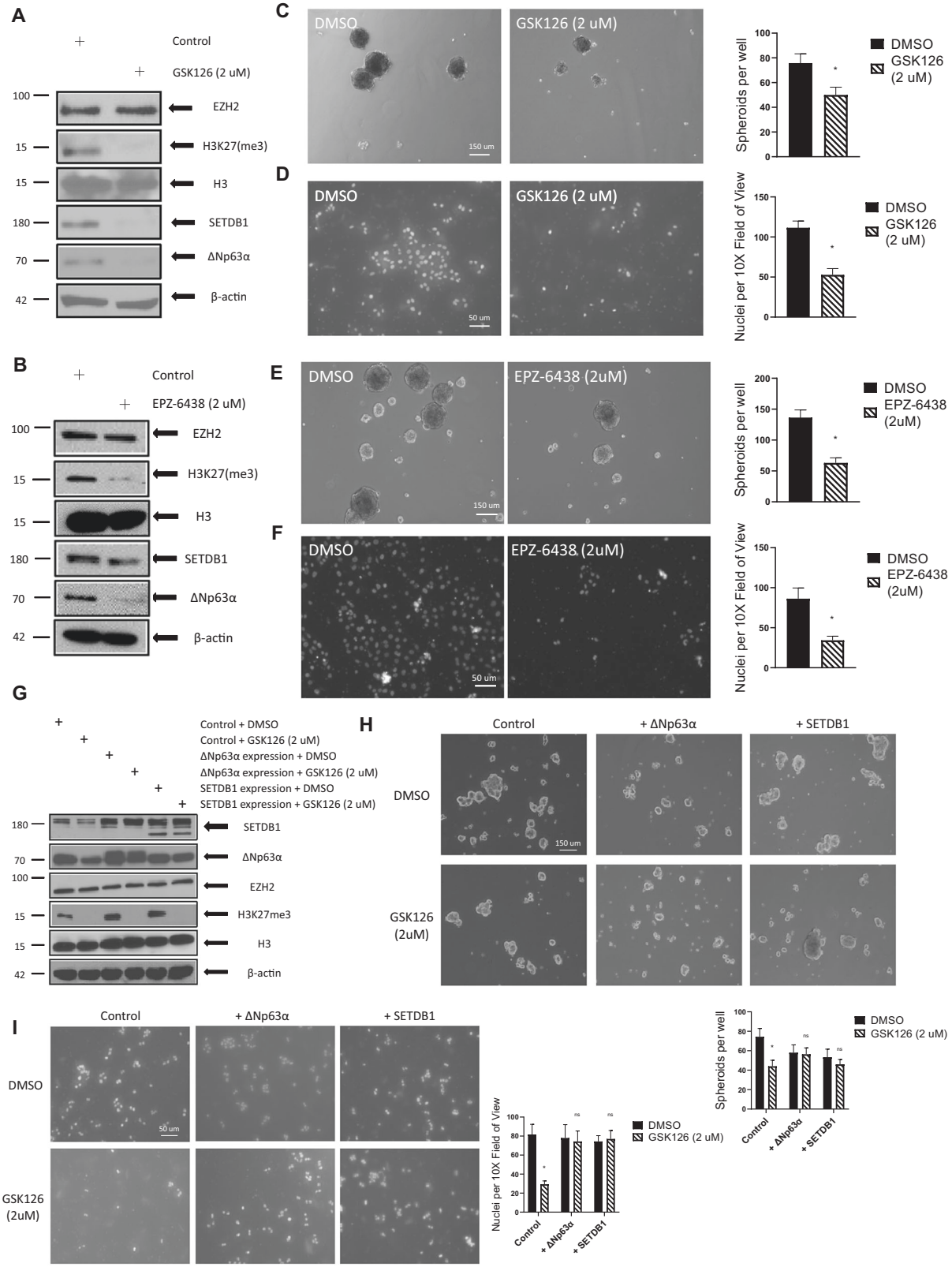

potential intermediate in the pathway that connects EZH2 to ΔNp63α and SETDB1, we performed RNA-seq from control and EZH2-depleted HSC-5 cells. EZH2 depletion led to decreased *TP63* RNA expression, but no change in *SETDB1* transcript levels, indicating that EZH2 affects SETDB1 strictly at the level of protein expression, whereas ΔNp63α is impacted at both the mRNA and protein level. We found that *RUNX3* was robustly upregulated in EZH2-depleted cells, contrasting the observed *TP63* decrease (Fig. 6A). RUNX3 is a transcription factor belonging to the runt domain-containing family of proteins [39] that is frequently studied as a

Fig. 5 The catalytic function of EZH2 is necessary for the regulation of SETDB1 and ΔNp63α. A HSC-5 cells were treated with the EZH2 inhibitor, GSK126, at a concentration of 2 uM for 48 h. Protein lysates were collected and western blotting was conducted for EZH2, tri-methyl H3K27 (a mark of EZH2 activity), SETDB1, and ΔNp63α. **B** The same western blotting procedure was also conducted following treatment with a different EZH2 inhibitor, EPZ-6438. **C** HSC-5 cells were plated for spheroid formation and treated at the time of seeding with 2 uM GSK126. Spheroids were counted after 10 days of non-attachment growth. **D** HSC-5 cells were also plated for invasion with 2 uM GSK126 treatment being administered to the cells at the time of seeding. Cells invaded for 24 h before collection and imaging. **E**, **F** EPZ-6438 treatment was applied to HSC-5 cells in both spheroid formation and invasions assays, as described above. **G** ΔNp63α and SETDB1 cDNAs were expressed in HSC-5 cells to establish overexpression cell lines. The overexpression cell lines were treated with 2 μM GSK126 for 48 h, protein lysates were collected and western blotting was carried out for EZH2, tri-methyl H3K27, SETDB1, and ΔNp63α. ΔNp63α and SETDB1 overexpression cells were also plated for (**H**) spheroid growth and (**I**) invasion assays with or without GSK126 treatment. Student's *t* tests were used to measure statistical significance (ns not significant, $*p$ value < 0.05). The average of three biological experiments is plotted for each experiment. Each biological replicate was run in triplicate.

tumor suppressor [28]. Notably, RUNX3 has also been observed in an oncogenic role in some cancers [40, 41]. In SCC in general, the literature is conflicting [42–45]. Recent literature suggests the oncogenic role of RUNX3 may be influenced by phosphorylation [46, 47].

Given *RUNX3* was robustly upregulated in HSC-5 cells when oncogenic EZH2 was depleted, RUNX3 was an ideal candidate to study as a potential tumor suppressor in the context of this novel signaling pathway. Literature implicating EZH2 as a direct regulator of tumor suppressive *RUNX3* further boosted the candidacy of RUNX3 as a point of focus [48].

First, RT-qPCR in EZH2-depleted HSC-5 cells confirmed the RNA-seq results for *TP63* and *SETDB1*. Primers were used specifically for *ΔNp63* isoforms of p63. EZH2 depletion caused a greater than 2-fold reduction in *ΔNp63*, while *SETDB1* expression did not change. GSK126 treatment of HSC-5 cells followed by RT-qPCR confirmed the effect on *ΔNp63* and *SETDB1* (Fig. 6B). In this case we can surmise that EZH2 impacts *ΔNp63* mRNA through its methyltransferase function. These findings were corroborated in Cal33 and FaDu cells, as *ΔNp63* was downregulated following GSK126 or EPZ-6438 treatment (Supplementary Fig. 5G).

To validate the effect of EZH2 depletion on *RUNX3* expression, we performed RT-qPCR from EZH2-depleted HSC-5 cells as well as from HSC-5 cells following GSK126 treatment. In both cases, *RUNX3* was significantly upregulated compared to control cells, and GSK126 treatment yielded a greater than 8-fold increase in *RUNX3* mRNA (Fig. 6C). We also assessed *RUNX3* mRNA in Cal33 and FaDu cell lines following EZH2 inhibition via GSK126 or EPZ-6438 treatment. *RUNX3* was significantly upregulated following EZH2 inhibition in both cell lines (Supplementary Fig. 5H). We also looked at the effect of EZH2 disruption on RUNX3 protein expression and observed a significant increase in RUNX3 following either genetic or pharmacological inhibition of EZH2 (Fig. 6D, E). Treatment with GSK126 or EPZ-6438 also increased RUNX3 protein in Cal33 and FaDu cells (Supplementary Fig. 5A).

To test the impact of specifically activating RUNX3 in SCC, we implemented a CRISPR activation system (CRISPRa) [49, 50]. An sgRNA for *ASCL1* and 2 sgRNAs for *NEUROG1* were used for positive controls to test the CRISPRa system in HSC-5 cells. Each sgRNA provided a robust upregulation of its intended target, as measured by RT-qPCR analysis (Fig. 6F). We then induced endogenous *RUNX3* expression using two sgRNAs targeted near the transcriptional start site for the P2 RUNX3 promoter [51], as *RUNX3* transcripts expressed from this promoter were significantly upregulated in our RNA-seq data. RT-qPCR analysis was conducted to test for successful *RUNX3* upregulation in our CRISPRa system, indicating that each sgRNA caused an increase in *RUNX3* expression greater than twofold. Furthermore, RT-qPCR analysis for *ΔNp63* showed that RUNX3-activated cells had significantly decreased *ΔNp63* expression (Fig. 6G). Protein expression of ΔNp63α, SETDB1, and EZH2 was then examined in RUNX3-activated HSC-5 cells, with ΔNp63α and SETDB1 decreasing following RUNX3 enrichment, whereas EZH2 expression remained constant (Fig. 6H), consistent with RUNX3 being downstream of EZH2 and functioning to repress ΔNp63α and SETDB1. As a repressor of ΔNp63α and SETDB1, we also looked at the effect of RUNX3 activation on spheroid formation and invasion. RUNX3 activation significantly impaired spheroid formation and invasion compared to controls (Fig. 6I, J).

To corroborate the impact of RUNX3 activation on SCC resulting from CRISPRa, we also expressed RUNX3 cDNA in HSC-5 cells and confirmed RUNX3 enrichment by western blot. Elevated RUNX3 also compromised ΔNp63α and SETDB1 expression (Fig. 7A). RT-qPCR in RUNX3-expressing cells confirmed the *RUNX3* increase, showed a decrease in *ΔNp63*, and showed no significant change in *SETDB1* mRNA (Fig. 7B). Furthermore, RUNX3-expressing cells were assayed for spheroid formation and invasion, demonstrating that elevated RUNX3 significantly impaired both phenotypes (Fig. 7C, D). Each of these findings were confirmed in FaDu and Cal33 cells, showing that RUNX3 expression: (1) compromised ΔNp63α and SETDB1 protein levels (Supplementary Fig. 6A); (2) increased *RUNX3* expression while reducing *ΔNp63* expression at the transcript level (Supplementary Fig. 6B) and; (3) significantly hampered both spheroid formation and invasion (Supplementary Fig. 6C, D). Lastly, due the emerging connections between RUNX3 function and p53 status, a possible role for p53 was examined in modulating the behavior of RUNX3 in this pathway [52]. Given that HSC-5 contains wild-type p53 while FaDu and Cal33 contain mutant p53, it is unlikely p53 plays a role in regulating RUNX3's tumor suppressive effect on SETDB1 and ΔNp63α [53]. To confirm that p53 was not assisting RUNX3's tumor suppressive function on this pathway, CRISPR was used to deplete p53, followed by RUNX3 overexpression. With reduced p53, RUNX3 was still able to repress SETDB1 and ΔNp63α in HSC-5 cells (Supplementary Fig. 7A).

We also examined RUNX3 family members, *RUNX1* and *RUNX2* following RNA-seq. Neither *RUNX1* nor *RUNX2* was upregulated in HSC-5 cells following CRISPR depletion of EZH2 (Supplementary Fig. 7B). This was confirmed via RT-qPCR following EZH2 inhibition. In FaDu and Cal33 cells, *RUNX1* also endured no significant change following EZH2 inhibition, however a modest upregulation of *RUNX2* was observed. Whether or not *RUNX2* is a direct EZH2 target and whether or not RUNX2 impacts SCC phenotypes in these cell lines warrants future study.

EZH2, SETDB1, and p63 are overexpressed in human SCCs

To further verify the role of EZH2, ΔNp63α, and SETDB1 in SCC and stem-like cancer cells, we performed IHC to stain for these oncoproteins in human SCCs. All three proteins stained more robustly in SCCs of the larynx, tongue, and nasal cavity, than in healthy tissue (Fig. 8A). Additionally, each of these proteins had the strongest expression in the basal layer, with decreased expression in more differentiated cells (Fig. 8B). The basal layer retains the stem cell population of SCCs, as indicated by increased SOX2 expression. Thus, robust expression of each of these proteins in SCC with enhanced expression in the basal layer confirms the relevance of EZH2-ΔNp63α-SETDB1 signaling in SCC cells that display stem cell markers.

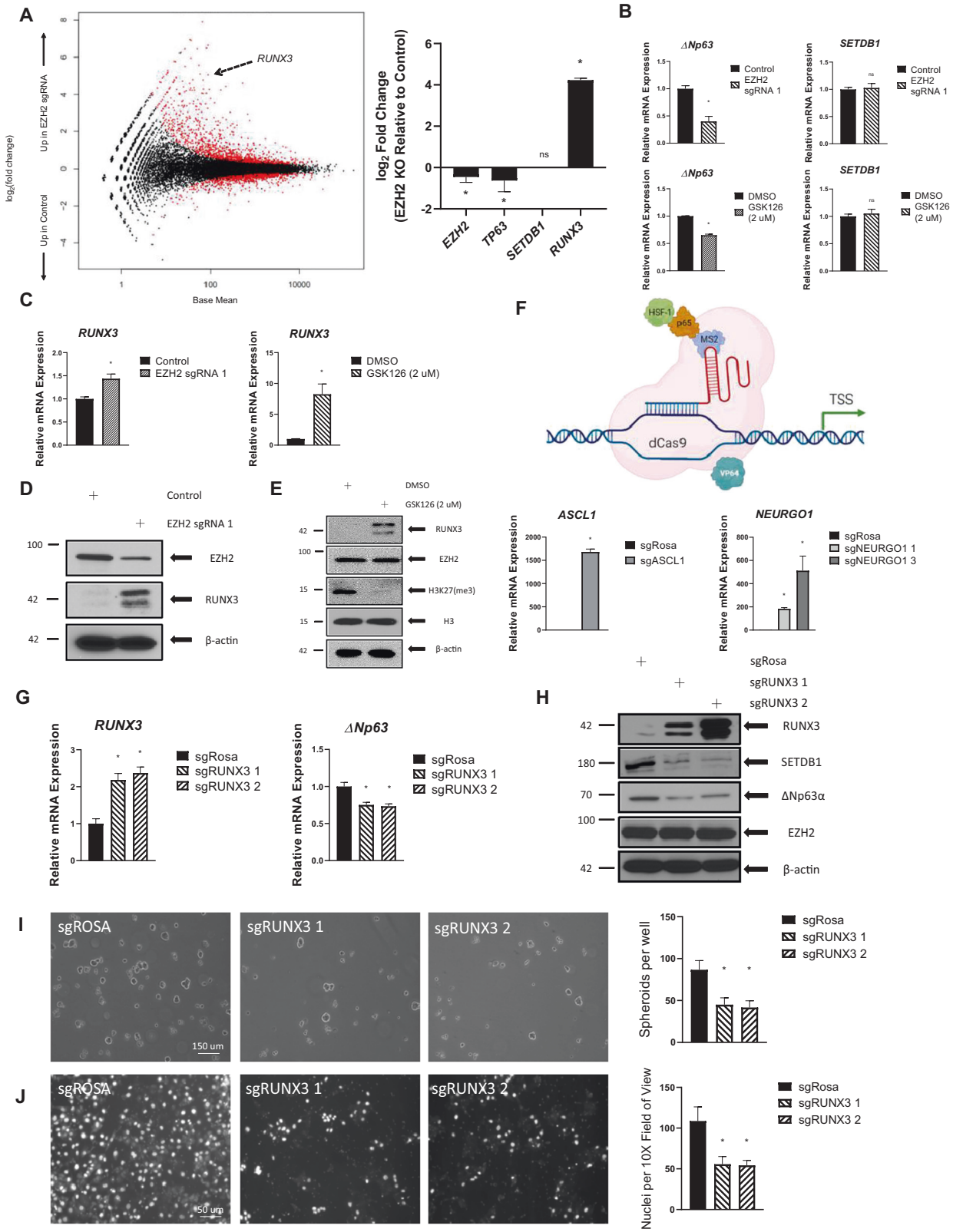

DISCUSSION

Evidence has continued to build in support of cancer stem cells (CSCs) as drivers of an advanced squamous cell carcinoma (SCC) disease state, contributing to phenotypes such as tumor initiation, metastasis, and treatment resistance [54]. In previous work, we demonstrate that non-attachment (spheroid) growth of SCC cells enriches for a stem-like sub-population of cancer cells that are highly invasive, migratory, and produce large, aggressive tumors in vivo [14]. We also show that the oncogenic isoform of p63, ΔNp63α, is an essential transcription factor that maintains this

Fig. 6 EZH2-repressed RUNX3 represses SETDB1 and ΔNp63α, and the SCC CSC phenotype. A RNA-seq was performed using RNA collected from HSC-5 control and EZH2 CRISPR-depleted cells. Differential expression analysis was performed and an MA plot was generated to visualize the differences in gene expression between control and EZH2-depleted cells (left). Log_2 fold changes were also calculated for *EZH2, TP63, SETDB1*, and *RUNX3* (right). **B** RT-qPCR was used to assess changes in *ΔNp63* and *SETDB1* mRNA following CRISPR-mediated depletion of EZH2 in HSC-5 cells (top). *ΔNp63* and *SETDB1* mRNA abundance was also looked at following 48 h of 2 uM GSK126 treatment (bottom). **C** RT-qPCR was also used to assess *RUNX3* mRNA abundance following CRISPR-mediated depletion of EZH2 (left), and GSK126 treatment (right). **D** RUNX3 protein expression was also examined by western blotting following CRISPR-mediated EZH2 depletion, or (**E**) GSK126 treatment. **F** A catalytically-null Cas9 enzyme (dCas9), equipped with coactivators, was stably expressed in HSC-5 cells, to establish a CRISPR activation (CRISPRa) system (top) (Created with BioRender.com). A sgRNA for *ASCL1* and 2 sgRNAs for *NEURGO1* were expressed in HSC-5 CRISPRa cells as positive controls. RT-qPCR was implemented to confirm overexpression of the endogenous genes (bottom). **G** 2 sgRNAs targeting *RUNX3* were expressed in the CRISPRa cells, and *RUNX3* mRNA expression was examined by RT-qPCR (left). RT-qPCR was also used to look at *ΔNp63* mRNA (right). **H** Protein lysates were collected from the RUNX3-activated HSC-5 cells and western blotting was performed for RUNX3, ΔNp63α, SETDB1, and EZH2. RUNX3-activated cells were also plated for (**I**) spheroid formation and (**J**) invasion assays. Student's *t* tests were used to measure statistical significance (ns not significant, **p* value < 0.05). The average of three biological experiments is plotted for each experiment. Each biological replicate was run in triplicate.

aggressive cell population, and its corresponding CSC phenotype. Here, we build on this work by identifying the histone H3K9 methyltransferase SETDB1 as vital to SCC. Consistent with SETDB1 directly binding ΔNp63α in breast cancer [22], we define the SETDB1-ΔNp63α interaction as essential to the SCC CSC phenotype. Lastly, we highlight RUNX3 as a key mediator of EZH2-dependent ΔNp63α/SETDB1 signaling. This pathway emerges as a promising target for clinical exploitation, given its essentiality to the SCC CSC phenotype and the availability of therapeutics that effectively inhibit EZH2 [27].

We initially identified SETDB1 and EZH2 as ideal targets for study through a small-scale, domain-focused CRISPR screen in which the functional domains of ~200 chromatin regulators are targeted [31]. *SETDB1* and *EZH2* scored as vulnerabilities in HSC-5 cells. By contrast, data from DepMap (https://depmap.org/portal) did not identify *SETDB1* or *EZH2* as a genetic dependency in HSC-5 cells, highlighting potentially additive value of focused domain-specific screens. Targeting the SET domains of SETDB1 and EZH2 yields a significant impact on the proliferation of HSC-5 cells as shown in our CRISPR screen data. We confirmed this effect with individual sgRNAs in HSC-5, FaDu and Cal33 cell lines. Further study using this approach is required to draw larger conclusions about the roles of the SET domains of EZH2 and SETDB1 in SCC overall.

In investigating the link between ΔNp63α and SETDB1, we show that these two proteins cooperate to maintain SCC. Additionally, both targets are robustly expressed in human SCC compared to healthy tissue. Furthermore, we show that each target regulates the other, such that a reduction in SETDB1 decreases ΔNp63α expression, and vice versa. Additionally, our data suggests distinct modes of regulation between these two factors. SETDB1 depletion reduces both ΔNp63α protein and mRNA, indicating a possible role for SETDB1 in regulating *ΔNp63* transcription and/or *ΔNp63*α mRNA stability. This is likely to be an indirect mode of regulation, considering the canonical repressive H3K9 methyltransferase function of SETDB1 at target loci. This presents the possibility that SETDB1 represses antagonists of *ΔNp63* transcription and/or antagonists of *ΔNp63* transcript stability, such as miRNAs [55]. While this may be a likely explanation, it remains possible that SETDB1 exerts its stabilizing effect at the protein level. Previous literature has shown ΔNp63 to transcriptionally regulate its own expression [36, 37]; therefore, SETDB1-mediated regulation of ΔNp63α protein might compromise *ΔNp63* mRNA by virtue of inhibiting ΔNp63α's positive feedback on its own promoter. Meanwhile, we show that ΔNp63α regulates SETDB1 strictly at the protein level, as p63 does not bind the *SETDB1* locus, and CRISPR-mediated ΔNp63α depletion does not significantly impact *SETDB1* mRNA abundance. This strongly supports a mode of protein regulation for ΔNp63α-mediated SETDB1 regulation. However, treatment of ΔNp63α-depleted cells with the proteasome inhibitor MG132 failed to rescue SETDB1 loss, implying a non-proteasomal mode of SETDB1 stabilization via ΔNp63α. Further study to elucidate the precise mechanism of SETDB1 protein stabilization by ΔNp63α will be helpful to fully delineate the relationship between these two proteins.

We further build on the ΔNp63α/SETDB1 connection by depleting each target and then showing that rescue of the other is sufficient to restore spheroid formation and invasion. Thus, SETDB1 and ΔNp63α not only affect overlapping biological phenotypes of SCC, but they do so in a manner that is dependent upon their reciprocal regulation. In addition to this, we demonstrate that CRISPR-mediated depletion of either target yields a significant reduction in tumorigenesis. Consequently, we elucidate a critical relationship between two oncoproteins that drive CSC phenotypes in SCC in a manner that is dependent upon their reciprocal regulation. To pursue methods of disrupting ΔNp63α-SETDB1 signaling and its corresponding SCC phenotypes, we sought upstream regulators of these targets that have existing small molecule inhibitors.

The H3K27 methyltransferase EZH2 is an essential gene based on our domain-focused CRISPR screening, which we connect to ΔNp63α via STAT3 methylation in previous work [14]. This, combined with the availability of small molecule inhibitors for EZH2 [27], makes it an ideal candidate to study in connection to ΔNp63α-SETDB1 signaling in SCC. As the catalytic component of PRC2, EZH2 exerts a repressive effect on target genes through mono- di- and tri-methylation of the histone H3-K27 residue [24]. In addition to showing that EZH2 depletion has a deleterious effect on monolayer cell proliferation, we also connected EZH2 to the SCC CSC phenotype. Spheroid formation and invasion are diminished upon EZH2 disruption, both by CRISPR-mediated depletion and by pharmacological inhibition using two different small molecules. Critically, EZH2 also affects ΔNp63α and SETDB1 expression, as genetic depletion of EZH2 compromises ΔNp63α and SETDB1 protein expression. Pharmacological inhibition of EZH2 enzymatic activity also decreases ΔNp63α and SETDB1, indicating that the methyltransferase function of EZH2 is necessary for the expression of these oncoproteins. *ΔNp63* mRNA also decreases following both genetic and pharmacological EZH2 perturbation. *SETDB1* mRNA abundance is not changed, as EZH2 regulates SETDB1 only at the protein level, comparable to what we observe following ΔNp63α depletion. Reintroduction of either SETDB1 or ΔNp63α into EZH2-depleted cells by cDNA overexpression provides robust rescue of both spheroid formation and invasion. In addition to rescuing EZH2 depletion, both SETDB1 and ΔNp63α are sufficient to nullify the impact of pharmacological inhibition of EZH2 on both spheroid formation and invasion.

To determine whether EZH2-mediated regulation of ΔNp63α and SETDB1 requires its canonical H3K27 methyltransferase function, we performed RNA-seq from EZH2-depleted SCC cells to identify changes in the transcriptome. *RUNX3*, which encodes a member of the runt domain-containing family of transcription factors [39], is robustly upregulated upon EZH2 depletion. As a

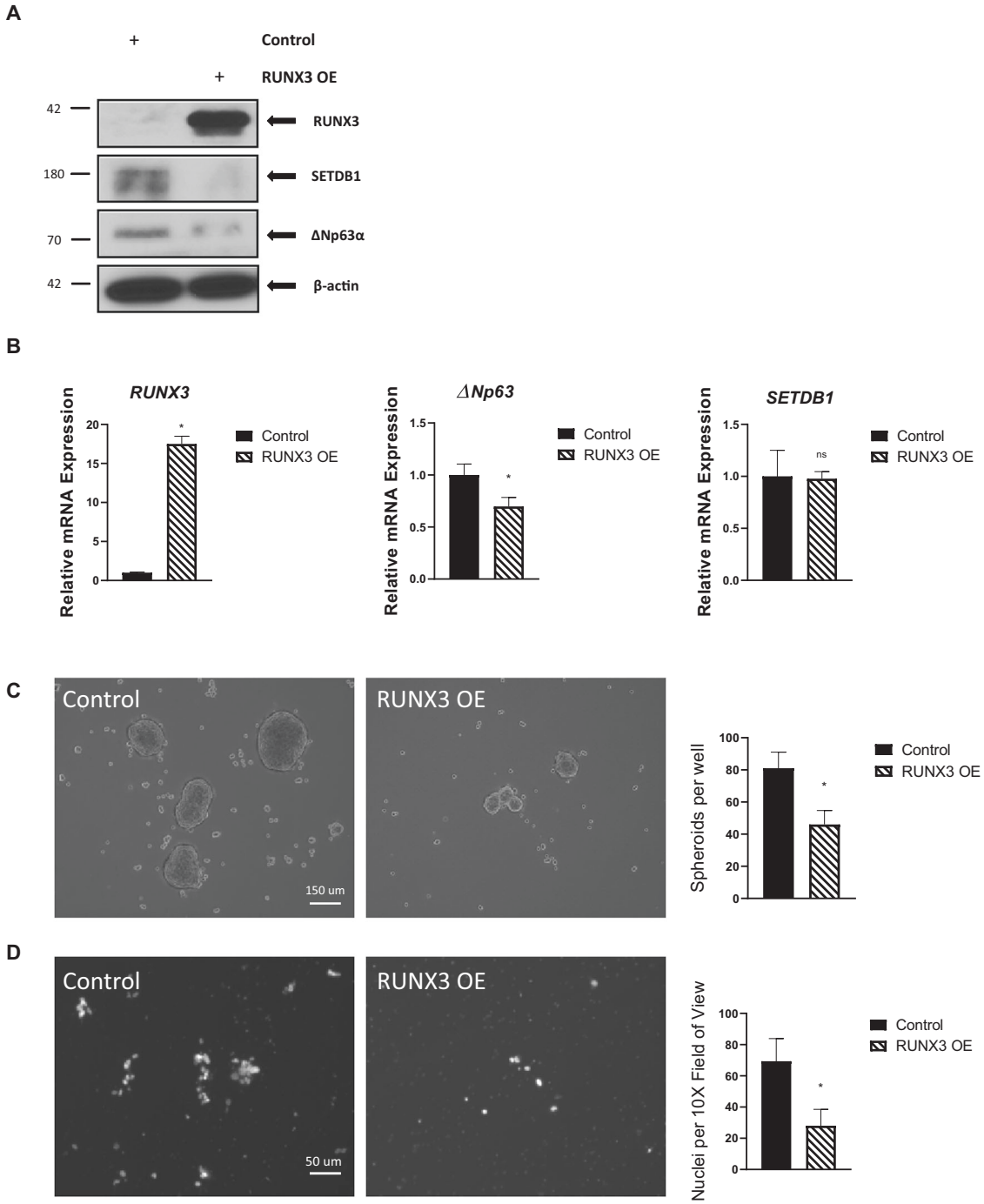

Fig. 7 RUNX3 is a repressor of ΔNp63α and SETDB1. A RUNX3 cDNA was overexpressed in HSC-5 cells and western blotting was used to confirm RUNX3 overexpression (OE), as well as to identify changes in SETDB1 and ΔNp63α. **B** RNA was collected from RUNX3 OE cells and RT-qPCR was used to detect changes in *RUNX3, SETDB1*, and *ΔNp63* mRNA. **C** RUNX3 OE HSC-5 cells were plated for a spheroid formation assay and total spheroids were counted following 10 days of growth. **D** RUNX3 OE cells were also plated for invasion and counted after 24 h. Student's *t* tests were used to measure statistical significance (ns not significant, **p* value < 0.05). The average of three biological experiments is plotted for each experiment. Each biological replicate was run in triplicate.

target of EZH2 [48], RUNX3 has a tumor suppressive effect in several cancers [28, 29, 43–45]. Yet in other cancers, RUNX3 has been reported to serve an oncogenic role [40–42]. Given the fact that EZH2 plays an oncogenic role in the cell lines examined here, and that *RUNX3* is robustly upregulated following EZH2 depletion or inhibition, it is likely that RUNX3 acts as a tumor suppressor in HSC-5, FaDu, and Cal33 SCC cell lines. This conclusion is supported by our findings that RUNX3 activation using two distinct methods inhibits the SCC CSC phenotype. The first method activates endogenous *RUNX3* expression via CRISPRa, in which a catalytically-null Cas9 enzyme is equipped with coactivators and directed to the endogenous *RUNX3* TSS via two different sgRNAs. The second method of RUNX3 activation occurs via lentiviral expression of *RUNX3* cDNA. Both of these approaches to activate RUNX3 expression lead to compromised expression of both SETDB1 and ΔNp63α. Furthermore, RUNX3 activation significantly

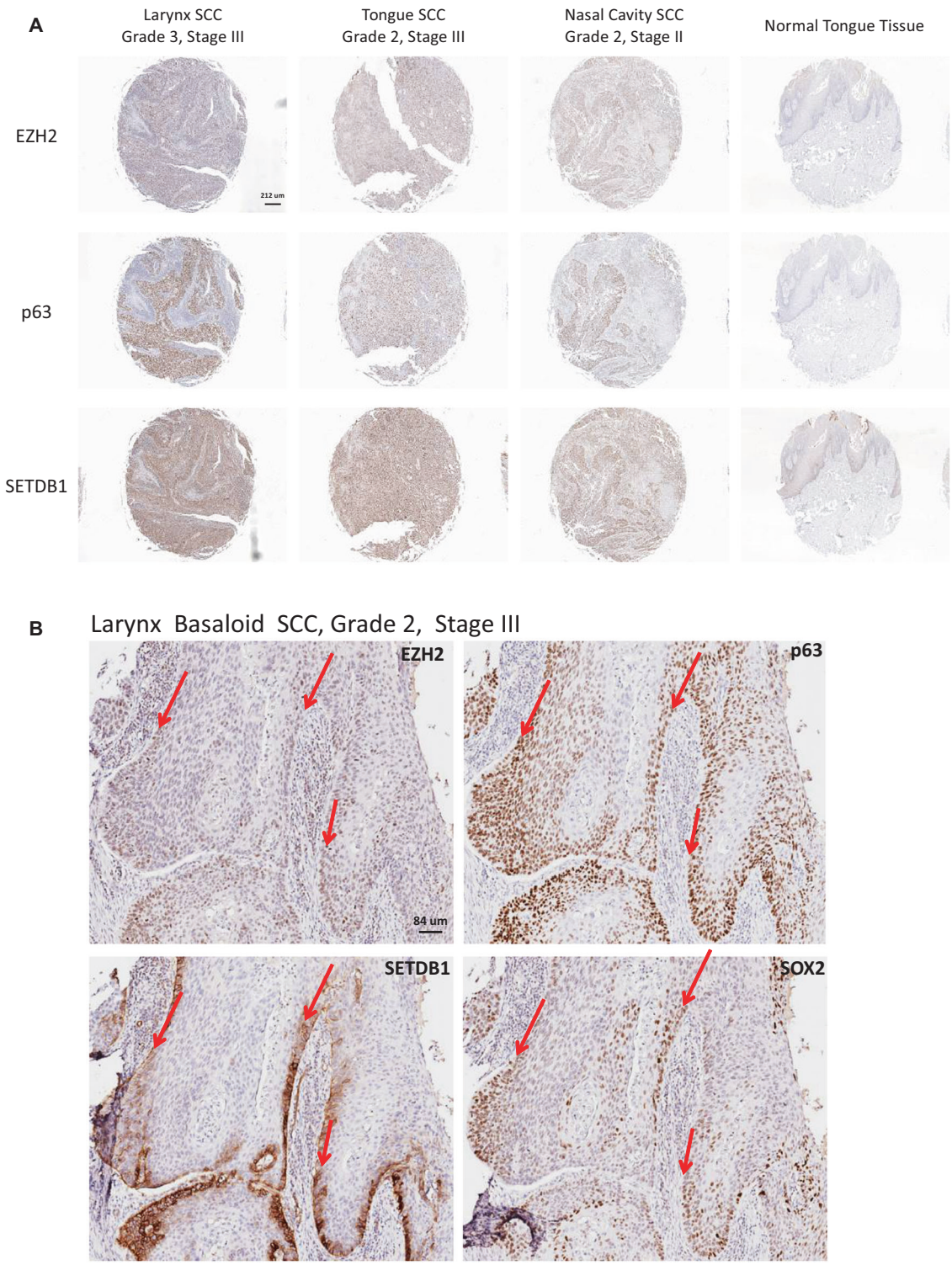

Fig. 8 EZH2, SETDB1 and p63 are overexpressed in human SCCs, and showed increased staining in cells with high SOX2 expression. **A** EZH2, SETDB1, and p63 anitbodies were used to stain tissue sections obtained from Biomax tumor microarrays. A Larynx SCC (grade 3, stage III), a tongue SCC (grade 2, stage III), and a nasal cavity SCC (grade 2, stage II) were looked at in comparison to healthy head and neck tissue (tongue). **B** Staining was also performed using the stem cell marker, SOX2, to highlight the basal layer in a grade 2 basaloid SCC of the larynx. This was compared to EZH2, SETDB1, and p63. Red arrows denote regions of SOX2-positive cell populations.

decreases both spheroid formation and invasion, as expected for a protein that represses ΔNp63α and SETDB1. Taken together, our findings highlight a crucial downstream target of EZH2 repression that, when activated, exerts a tumor suppressive effect in SCC via repression of the ΔNp63α/SETDB1-driven CSC phenotype.

This work delineates a novel EZH2-RUNX3-ΔNp63α-SETDB1 signaling pathway that influences an aggressive cancer stem cell phenotype of SCC. This axis holds potential as a viable clinical target considering the availability of EZH2 inhibitors, and our data highlights the fact that the oncogenic components of this

pathway are elevated in SCC patient samples, particularly within the basal layer where there is high SOX2 expression marking the stem cell population. This corroborates our cell-based studies that show the necessity of each of these proteins in maintaining properties associated with stem-like SCC cells. In this study, we demonstrate a means of targeting ΔNp63α and SETDB1-driven human SCCs via EZH2 inhibition, and subsequent RUNX3 activation. Future studies will more fully define the mechanisms connecting ΔNp63α and SETDB1, as well as to elucidate the role of RUNX3 as a tumor suppressor within the cancer stem cell population of SCC.

MATERIALS AND METHODS

Cell culture and lentivirus production

Cell culture was performed and lentivirus was produced as previously described [14]. Human HSC-5 cells were obtained from Sekisui Xenotech, LLC (Kansas City, KS), and human FaDu and Cal-33 cell lines were a generous gift from Leif Ellison. All cell lines tested negative for Mycoplasma contamination using Myco Alert (LT07-218) from Lonza (Basel, CH).

Western blotting

For immunoblot analyses, equivalent amounts of protein were electrophoresed on denaturing and reducing 10% polyacrylamide gels and transferred to nitrocellulose membrane. Membranes were blocked by 5% nonfat dry milk and then incubated with the appropriate primary (1:1000) and secondary antibodies (1:5000). Secondary antibody binding was visualized using chemiluminescence detection technology. Biological triplicates were run for each blot.

Quantitative RT-PCR

Total RNA was isolated with the RNAspin Mini Kit (GE Healthcare) and reverse transcribed using the superscript III reverse transcriptase (Invitrogen, Carlsbad, CA). RNA (500 ng) was used for cDNA preparation. The Light Cycler 480 SYBR Green I Master mix (Roche Diagnostics) was used to measure mRNA. mRNA level was detected and signals were normalized to level of beta-Actin mRNA. Three biological replicates were run for each experiment, with technical triplicates of each. Data is plotted as the average of biological replicates.

Spheroid formation and invasion assays

Assays were performed as previously described [14]. Images were acquired using a Zeiss Axiovert LED microscope. Three biological replicates were run for each experiment, with technical triplicates of each. Data is plotted as the average of biological replicates.

Immunohistochemistry

Expression of EZH2, SETDB1, p63, and SOX2 was tested using tissue arrays of SCC samples from US Biomax (HN804 and HN802d), as previously described [14].

GSK126 and EPZ-6438 treatment

For western blotting and RT-qPCR: Cells were treated with either 2 μM GSK126 or EPZ-6438 for 24 h in DMEM containing 10% FBS. Following 24 h, the media was changed and 2 μM of fresh inhibitor was added. Protein and RNA were collected 24 h after the second treatment. DMSO (vehicle) was used as a control. For spheroid formation assays, inhibitors were added to spheroid media at the time of plating. For invasion assays, inhibitors were added to media in the upper compartment of the transwell insert at the time of seeding.

DATA AVAILABILITY

RNA-seq and ChIP-seq data are available from the Gene Expression Omnibus database (accession no. GSE202789) Methods for CRISPR activation, CRISPR depletion, domain-focused CRISPR screening, cDNA overexpression, EPZ-6438 and GSK126 treatment, GFP depletion assays, tumor xenografts, ChIP-seq, and RNA-seq are described in the Supplementary Information. Antibodies and reagents are also listed there, as well as RT-qPCR primer sequences and sgRNA sequences.

REFERENCES

1. Yan W, Wistuba II, Emmert-Buck MR, Erickson HS. Squamous cell carcinoma—similarities and differences among anatomical sites. Am J Cancer Res. 2011;1:275–300.
2. Paver EC, Currie AM, Gupta R, Dahlstrom JE. Human papilloma virus related squamous cell carcinomas of the head and neck: diagnosis, clinical implications and detection of HPV. Pathology. 2020;52:179–91.
3. Liu-Smith F, Jia J, Zheng Y. UV-induced molecular signaling differences in melanoma and non-melanoma skin cancer. Adv Exp Med Biol. 2017;996:27–40.
4. Kikuchi K, Inoue H, Miyazaki Y, Ide F, Kojima M, Kusama K. Epstein-Barr virus (EBV)-associated epithelial and non-epithelial lesions of the oral cavity. Jpn Dent Sci Rev. 2017;53:95–109.
5. Johnson N. Tobacco use and oral cancer: a global perspective. J Dent Educ. 2001;65:328–39.
6. Crosbie EJ, Einstein MH, Franceschi S, Kitchener HC. Human papillomavirus and cervical cancer. Lancet. 2013;382:889–99.
7. Bacciu A, Mercante G, Ingegnoli A, Ferri T, Muzzetto P, Leandro G, et al. Effects of gastroesophageal reflux disease in laryngeal carcinoma. Clin Otolaryngol Allied Sci. 2004;29:545–8.
8. Lee SH. Chemotherapy for lung cancer in the era of personalized medicine. Tuberc Respir Dis. 2019;82:179–89.
9. Deng HY, Wang WP, Wang YC, Hu WP, Ni PZ, Lin YD, et al. Neoadjuvant chemoradiotherapy or chemotherapy? A comprehensive systematic review and meta-analysis of the options for neoadjuvant therapy for treating oesophageal cancer. Eur J Cardiothorac Surg. 2017;51:421–31.
10. Tagliamento M, Genova C, Rijavec E, Rossi G, Biello F, Dal Bello MG, et al. Afatinib and Erlotinib in the treatment of squamous-cell lung cancer. Expert Opin Pharmacother. 2018;19:2055–62.
11. Kaidar-Person O, Gil Z, Billan S. Precision medicine in head and neck cancer. Drug Resist Updat. 2018;40:13–6.
12. Oshimori N. Cancer stem cells and their niche in the progression of squamous cell carcinoma. Cancer Sci. 2020;111:3985–92.
13. Dragu DL, Necula LG, Bleotu C, Diaconu CC, Chivu-Economescu M. Therapies targeting cancer stem cells: Current trends and future challenges. World J Stem Cells. 2015;7:1185–201.
14. Fisher ML, Balinth S, Hwangbo Y, Wu C, Ballon C, Wilkinson JE, et al. BRD4 regulates transcription factor ΔNp63α to drive a cancer stem cell phenotype in squamous cell carcinomas. Cancer Res. 2021;81:6246–58.
15. Mills AA, Zheng B, Wang XJ, Vogel H, Roop DR, Bradley A. p63 is a p53 homologue required for limb and epidermal morphogenesis. Nature. 1999;398:708–13.
16. Yang A, Kaghad M, Wang Y, Gillett E, Fleming MD, Dötsch V, et al. p63, a p53 homolog at 3q27-29, encodes multiple products with transactivating, death-inducing, and dominant-negative activities. Mol Cell. 1998;2:305–16.
17. Soares E, Zhou H. Master regulatory role of p63 in epidermal development and disease. Cell Mol Life Sci. 2018;75:1179–90.
18. Fisher ML, Balinth S, Mills AA. p63-related signaling at a glance. J Cell Sci. 2020;133:jcs228015.
19. Petitjean A, Ruptier C, Tribollet V, Hautefeuille A, Chardon F, Cavard C, et al. Properties of the six isoforms of p63: p53-like regulation in response to genotoxic stress and cross talk with DeltaNp73. Carcinogenesis. 2008;29:73–81.
20. Ayyanathan K, Lechner MS, Bell P, Maul GG, Schultz DC, Yamada Y, et al. Regulated recruitment of HP1 to a euchromatic gene induces mitotically heritable, epigenetic gene silencing: a mammalian cell culture model of gene variegation. Genes Dev. 2003;17:1855–69.
21. Karanth AV, Maniswami RR, Prashanth S, Govindaraj H, Padmavathy R, Jegatheesan SK, et al. Emerging role of SETDB1 as a therapeutic target. Expert Opin Ther Targets. 2017;21:319–31.
22. Regina C, Compagnone M, Peschiaroli A, Lena A, Annicchiarico-Petruzzelli M, Piro MC, et al. Setdb1, a novel interactor of ΔNp63, is involved in breast tumorigenesis. Oncotarget. 2016;7:28836–48.
23. Margueron R, Reinberg D. The Polycomb complex PRC2 and its mark in life. Nature. 2011;469:343–9.
24. Bachmann IM, Halvorsen OJ, Collett K, Stefansson IM, Straume O, Haukaas SA, et al. EZH2 expression is associated with high proliferation rate and aggressive tumor subgroups in cutaneous melanoma and cancers of the endometrium, prostate, and breast. J Clin Oncol. 2006;24:268–73.
25. Sneeringer CJ, Scott MP, Kuntz KW, Knutson SK, Pollock RM, Richon VM, et al. Coordinated activities of wild-type plus mutant EZH2 drive tumor-associated hypertrimethylation of lysine 27 on histone H3 (H3K27) in human B-cell lymphomas. Proc Natl Acad Sci USA. 2010;107:20980–5.
26. Zhao M, Hu X, Xu Y, Wu C, Chen J, Ren Y, et al. Targeting of EZH2 inhibits epithelial-mesenchymal transition in head and neck squamous cell carcinoma via regulating the STAT3/VEGFR2 axis. Int J Oncol. 2019;55:1165–75.
27. Kim KH, Roberts CW. Targeting EZH2 in cancer. Nat Med. 2016;22:128–34.

28. Bae SC, Choi JK. Tumor suppressor activity of RUNX3. Oncogene. 2004;23:4336–40.
29. Xiao Z, Tian Y, Jia Y, Shen Q, Jiang W, Chen G, et al. RUNX3 inhibits the invasion and migration of esophageal squamous cell carcinoma by reversing the epithelial-mesenchymal transition through TGF-β/Smad signaling. Oncol Rep. 2020;43:1289–99.
30. Keyes WM, Pecoraro M, Aranda V, Vernersson-Lindahl E, Li W, Vogel H, et al. ΔNp63α is an oncogene that targets chromatin remodeler Lsh to drive skin stem cell proliferation and tumorigenesis. Cell Stem Cell. 2011;8:164–76.
31. Shi J, Wang E, Milazzo JP, Wang Z, Kinney JB, Vakoc CR. Discovery of cancer drug targets by CRISPR-Cas9 screening of protein domains. Nat Biotechnol. 2015;33:661–7.
32. Sniezek JC, Matheny KE, Westfall MD, Pietenpol JA. Dominant negative p63 isoform expression in head and neck squamous cell carcinoma. Laryngoscope. 2004;114:2063–72.
33. Somerville TDD, Xu Y, Miyabayashi K, Tiriac H, Cleary CR, Maia-Silva D, et al. TP63-mediated enhancer reprogramming drives the squamous subtype of pancreatic ductal adenocarcinoma. Cell Rep. 2018;25:1741–55.e7.
34. Bailey TL, Johnson J, Grant CE, Noble WS. The MEME Suite. Nucleic Acids Res. 2015;43:W39–49.
35. Kent WJ, Sugnet CW, Furey TS, Roskin KM, Pringle TH, Zahler AM, et al. The human genome browser at UCSC. Genome Res. 2002;12:996–1006.
36. Romano RA, Birkaya B, Sinha S. Defining the regulatory elements in the proximal promoter of DeltaNp63 in keratinocytes: Potential roles for Sp1/Sp3, NF-Y, and p63. J Investig Dermatol. 2006;126:1469–79.
37. Antonini D, Rossi B, Han R, Minichiello A, Di Palma T, Corrado M, et al. An autoregulatory loop directs the tissue-specific expression of p63 through a long-range evolutionarily conserved enhancer. Mol Cell Biol. 2006;26:3308–18.
38. Tsusaka T, Shimura C, Shinkai Y. ATF7IP regulates SETDB1 nuclear localization and increases its ubiquitination. EMBO Rep. 2019;20:e48297.
39. Bangsow C, Rubins N, Glusman G, Bernstein Y, Negreanu V, Goldenberg D, et al. The RUNX3 gene-sequence, structure and regulated expression. Gene. 2001;279:221–32.
40. Selvarajan V, Osato M, Nah GSS, Yan J, Chung TH, Voon DC, et al. RUNX3 is oncogenic in natural killer/T-cell lymphoma and is transcriptionally regulated by MYC. Leukemia. 2017;31:2219–27.
41. Otani S, Date Y, Ueno T, Ito T, Kajikawa S, Omori K, et al. Runx3 is required for oncogenic Myc upregulation in p53-deficient osteosarcoma. Oncogene. 2022;41:683–91.
42. Kudo Y, Tsunematsu T, Takata T. Oncogenic role of RUNX3 in head and neck cancer. J Cell Biochem. 2011;112:387–93.
43. Gao F, Huang C, Lin M, Wang Z, Shen J, Zhang H, et al. Frequent inactivation of RUNX3 by promoter hypermethylation and protein mislocalization in oral squamous cell carcinomas. J Cancer Res Clin Oncol. 2009;135:739–47.
44. Jili S, Eryong L, Lijuan L, Chao Z. RUNX3 inhibits laryngeal squamous cell carcinoma malignancy under the regulation of miR-148a-3p/DNMT1 axis. Cell Biochem Funct. 2016;34:597–605.
45. Sugiura H, Ishiguro H, Kuwabara Y, Kimura M, Mitsui A, Mori Y, et al. Decreased expression of RUNX3 is correlated with tumor progression and poor prognosis in patients with esophageal squamous cell carcinoma. Oncol Rep. 2008;19:713–9.
46. Kumar A, Singhal M, Chopra C, Srinivasan S, Surabhi RP, Kanumuri R, et al. Threonine 209 phosphorylation on RUNX3 by Pak1 is a molecular switch for its dualistic functions. Oncogene. 2016;35:4857–65.
47. Kanumuri R, Chelluboyina AK, Biswal J, Vignesh R, Pandian J, Venu A, et al. Small peptide inhibitor from the sequence of RUNX3 disrupts PAK1–RUNX3 interaction and abrogates its phosphorylation-dependent oncogenic function. Oncogene. 2021;40:5327–41.
48. Fujii S, Ito K, Ito Y, Ochiai A. Enhancer of zeste homologue 2 (EZH2) down-regulates RUNX3 by increasing histone H3 methylation. J Biol Chem. 2008;283:17324–32.
49. Lu B, Klingbeil O, Tarumoto Y, Somerville TDD, Huang YH, Wei Y, et al. A transcription factor addiction in leukemia imposed by the MLL promoter sequence. Cancer Cell. 2018;34:970–81.e8.
50. Konermann S, Brigham MD, Trevino AE, Joung J, Abudayyeh OO, Barcena C, et al. Genome-scale transcriptional activation by an engineered CRISPR-Cas9 complex. Nature. 2015;517:583–8.
51. Levanon D, Groner Y. Structure and regulated expression of mammalian RUNX genes. Oncogene. 2004;23:4211–9.
52. Date Y, Ito K. Oncogenic RUNX3: a link between p53 deficiency and MYC dysregulation. Mol Cells. 2020;43:176–81.
53. Jiang L, Yu H, Ness S, Mao P, Guo F, Tang J, et al. Comprehensive analysis of co-mutations identifies cooperating mechanisms of tumorigenesis. Cancers. 2022;14:415.
54. Jian Z, Strait A, Jimeno A, Wang XJ. Cancer stem cells in squamous cell carcinoma. J Investig Dermatol. 2017;137:31–7.
55. Lin C, Li X, Zhang Y, Guo Y, Zhou J, Gao K, et al. The microRNA feedback regulation of p63 in cancer progression. Oncotarget. 2015;6:8434–53.

ACKNOWLEDGEMENTS

This work was supported by the Office of the Director, National Institutes of Health through award numbers 5P30CA045508 (Cancer Center Support Grant), CA247400 (to SB), CA225134 (to MLF), as well as R01CA190997 and R21OD018332 (to AAM). This project was also supported through the Cold Spring Harbor Laboratory and Northwell Health Affiliation.

AUTHOR CONTRIBUTIONS

SB: Performed and designed experiments, paper writing. MLF: Performed and designed experiments. YH: Performed and designed experiments. CW: Performed and designed experiments. CB: Performed experiments. XS: Designed experiments. AAM: Experimental design and direction, paper writing, funding.

COMPETING INTERESTS

The authors declare no competing interests.

ADDITIONAL INFORMATION

Supplementary information The online version contains supplementary material available at https://doi.org/10.1038/s41388-022-02417-4.

Correspondence and requests for materials should be addressed to Alea A. Mills.